

Impact of Declining Arctic Sea Ice on Winter Snowfall

Jiping Liu¹ Judith A. Curry¹ Huijun Wang² Mirong Song² Radley M. Horton³

¹School of Earth & Atmospheric Sciences, Georgia Institute of Technology,
Atlanta, GA 30332, USA

²Institute of Atmospheric Physics, Chinese Academy of Sciences, Beijing, 100029, China

³Columbia University Center for Climate Systems Research,
New York, NY, 10025, USA

Abstract

While the Arctic region has been warming strongly in recent decades, anomalously large snowfall in recent winters has affected large parts of North America, Europe, and East Asia. Here we demonstrate that the decrease in autumn Arctic sea ice area is linked to changes in the winter Northern Hemisphere atmospheric circulation that have some resemblance to the negative phase of the winter Arctic Oscillation. However, the atmospheric circulation change linked to the reduction of sea ice shows much broader meridional meanders in mid-latitudes and clearly different interannual variability than the classical Arctic Oscillation. This circulation change results in more frequent episodes of blocking patterns that lead to increased cold surges over large parts of northern continents. Moreover, the increase in atmospheric water vapor content in the Arctic region during late autumn and winter driven locally by the reduction of sea ice provides enhanced moisture sources, supporting increased heavy snowfall in Europe during early winter, and the northeastern and mid-west United States during winter. We conclude that the recent decline of Arctic sea ice has played a critical role in recent cold and snowy winters.

1 \body

2 **Introduction**

3 During the past few winters, North America, Europe, and East Asia have experienced
4 anomalously cold conditions, along with record snowfalls (1-3). Anomalously heavy snowfall
5 wrought havoc in large parts of the United States and northwestern Europe for the winters of
6 2009/2010 and 2010/2011. A series of snowstorms hit central and southern China for the
7 winter of 2007/2008. Persistent snow, freezing rain, and cold temperature resulted in
8 disruptions in transport, energy supply and power transmission, and damage to agriculture (1-
9 3). The causes of the recent severe winters are unclear, particularly in context of the amplified
10 warming in the Arctic (4, 5) that has contributed to the reduction of sea ice.

11 Some explanations have been offered for the recent severe winters from the perspective of
12 dominant modes of climate variability. Seager et al. (6) suggest that the anomalously high
13 levels of snowfall in the mid-Atlantic states of the United States and northwestern Europe for
14 the winter of 2009/2010 were forced by the negative phase of the North Atlantic Oscillation
15 (NAO) and to a lesser extent by the El Niño. Ratnam et al. (7) show that the heating associated
16 with the El Niño Modoki during boreal winter 2009/2010 accounts for most of the anomalous
17 conditions observed over parts of North America and Europe. Cohen et al. (8) argue that the
18 strong negative Arctic Oscillation (AO, 9) for the winter of 2009/2010 is the major
19 contributing factor to severe winter weather in the Northern Hemisphere. As shown in
20 supplementary Fig. 1, significantly above-normal winter snow cover has been present in large
21 parts of the northern United States, northwestern and central Europe, and northern and central
22 China for the four winters since the record low Arctic sea ice during 2007. However, no clear
23 persistent out-of-phase NAO/AO-snow cover and in-phase El Niño-snow cover relationship
24 are evident in the observations for the past four winters (Supplementary Fig. 2). Diminishing
25 Arctic sea ice and its potential climatic impacts have received increasing attention (10-12), i.e.
26 many studies have demonstrated that regional loss of Arctic sea ice can have hemispheric
27 consequences in atmospheric circulation (13-19). Recent studies show that cold conditions and

1 increased snow cover over Siberia in autumn is correlated with reduced September sea ice
2 cover in the Pacific sector of the Arctic (20, 21). Furthermore, supplementary Fig. 2 does
3 support a persistent out-of-phase sea ice-snow cover relationship for the past four winters.

4 Here we extend previous studies by combining observational data analyses and numerical
5 experiments, demonstrating how anomalously large snowfall in large parts of the northern
6 hemisphere continents in recent winters are linked to diminishing Arctic sea ice.

7 **Results**

8 For the period of the available satellite data record (since the late 1970s), Arctic sea ice
9 extent has been decreasing in all months, with the most pronounced loss in September (22). As
10 shown in Fig. 1, the autumn (September-October-November) Arctic sea ice area has declined
11 27.3% for 1979-2010 (relative to the climatology, > 99% significance). In 2007, the autumn
12 Arctic sea ice area reached an unexpectedly low value, outpacing that simulated by IPCC AR4
13 climate models in response to greenhouse warming (23). Our speculation surrounding the
14 connection between the accelerated decline of Arctic sea ice for the past few years and recent
15 anomalously cold and snowy winters over northern continents is based on the following
16 mechanisms. When highly reflective sea ice is replaced by open water during the ice melting
17 period, there is a substantial solar heat input directly into the ocean, increasing the heat stored
18 in the upper ocean. For example, the cumulative solar heat input in the Beaufort Sea during
19 the ice melting period in 2007 can be a factor of two to five higher than climatology, which is
20 sufficient to warm the upper 5 m of the ocean by 5°C (24). The loss of sea ice in the Canada
21 basin has also been accompanied by the widespread appearance of a near-surface temperature
22 maximum at 25-35 m depth due to penetrating solar radiation (25). Warming of the upper
23 ocean retards the recovery of sea ice during the fall freeze-up. As a result, the ice coverage in
24 late autumn and early winter for the past few years is significantly below the mean of 1979-
25 2000, exceeding two standard deviation of ice variability (Supplementary Fig. 3). The
26 anomalously warm, ice-free ocean water increases the ocean surface flux of heat and moisture
27 into the atmosphere in late autumn and early winter, which in turn has substantial impacts on

1 winter atmospheric circulation.

2 By examining observational data for the period 1979-2010, the fraction of winter
3 (December-January-February) climate of the extra-tropical northern hemisphere that is
4 linearly congruent with the interannual variability of autumn Arctic sea ice is found by
5 regressing winter anomalies of snow cover, and atmospheric fields from the National Center
6 for Environmental Prediction reanalysis II (NCEP2) onto the detrended autumn Arctic sea ice
7 area. The regression map between sea ice area and snow cover reveals that snow cover
8 anomalies over the northern hemisphere continents are closely linked to Arctic sea ice
9 variability. A decrease of autumn Arctic sea ice of one million km² corresponds to a
10 significantly above-normal winter snow cover (> 3-12%) in large parts of the northern United
11 States, northwestern and central Europe, and northern and central China (Fig. 1B).

12 One important contributor to the anomalously large snowfall in recent winters is changes
13 in atmospheric circulation linked to diminishing Arctic sea ice. The regression map between
14 sea ice area and sea level pressure (SLP) reveals that following anomalously low ice coverage
15 in autumn, the winter SLP is substantially higher over the Arctic Ocean, the northern Atlantic,
16 and much of high-latitude continents, which is compensated by lower SLP in mid-latitudes
17 (Fig. 2A). This pattern shows some resemblance to the negative phase of the winter AO (Fig.
18 2B). However, some significant differences are noticed. First, the pattern linked to the
19 reduction of autumn sea ice shows broader meridional meanders in mid-latitudes rather than
20 the zonal symmetry associated with the winter AO pattern (Fig. 2A vs. 2B). A recent study
21 also noted that recent loss of summer sea ice in the Arctic is directly connected to a shift to a
22 more meridional atmospheric circulation pattern in the following autumn, and suggested that
23 increased modification of atmospheric circulation pattern would be anticipated with
24 continuing loss of summer sea ice to less than 20% of its climatology over the next decades
25 (26). Second, the pattern linked to the reduction of autumn sea ice shows clearly different
26 interannual variability relative to the classical winter AO pattern, i.e. the detrended autumn
27 Arctic sea ice and winter AO indices have weak correlation (0.28), only accounting for ~8%

1 of the shared variance. Thus, the atmospheric circulation change linked to the reduction of sea
2 ice is different from the classical AO.

3 Under such circulation change, the prevailing westerly winds blowing across the North
4 Atlantic (North Pacific) from Canada (offshore of Japan) to Europe (Canada) are weakened.
5 As shown in the vertical cross-section of the regression of the winter zonal mean zonal wind
6 anomalies on the detrended autumn Arctic sea ice area anomaly (Supplementary Fig. 4), the
7 zonal wind anomalies are negative in mid-latitudes extending from the surface to the
8 troposphere, which represent 20-60% of the magnitude of the climatological zonal wind. This
9 suggests a shift to a more meridional anomalous wind pattern in winter congruent with the
10 reduction of the autumn Arctic sea ice. Weak westerly winds tend to enhance broader
11 meanders that are likely to form blocking circulations. Fig. 3A shows that associated with the
12 reduction of autumn sea ice, there is an increased incidence of blockings during winter over
13 much of northern high-latitude continents, with the most pronounced increase in eastern
14 Europe, central Siberia, southern Alaska and the northwestern United States (20-60% greater
15 than climatology). These blocking patterns favor more frequent incursions of cold air masses
16 from the Arctic into mid- and low-latitude of northern continents. As shown in Fig. 3B, there
17 is an increased frequency of cold events over much of northern continents, with the most
18 pronounced increase in the eastern and mid-west United States, northwestern Europe, between
19 mid-East and central Asia, and central and south China (20-60% greater than climatology).
20 This leads to cold conditions over much of northern continents, i.e. temperature anomalies
21 extending southeastward from northwestern Canada to the southeastern United States, and
22 eastward/southeastward from northwestern Europe to central China can be 2-3°C below-
23 normal in association with one million km² decrease of the autumn Arctic sea ice (Fig. 2C).

24 The only notable exception is northeastern Canada and Greenland, where weak westerly
25 winds favors more frequent incursions of warm air masses from the North Atlantic. This leads
26 to warm anomalies there (Fig. 2C), helping to explain extremely low ice coverage observed in
27 Baffin/Hudson Bay, Davis Strait, the Labrador Sea, and Gulf of Saint Lawrence in recent

winters, particularly in 2009/2010 and 2010/2011 (Supplementary Fig. 5).

Another potential contributor to anomalously large snowfall in recent winters is changes in atmospheric water vapor content over northern high-latitudes. The rapid retreat of sea ice in summer and slow recovery of sea ice in autumn, particularly after 2007, greatly enhances moisture flux from the ocean to the atmosphere. This increases the humidity of Arctic air masses remarkably during ice growth period. Following anomalously low ice coverage in autumn, the regions with the most pronounced increase of specific humidity (integrated from surface to 700-hPa) during late autumn and early winter are found in northern/eastern Europe, far eastern Siberia and western Alaska (Fig. 3C). During winter, the regions showing the most pronounced increase of specific humidity mainly shift to northeastern North America due to the aforementioned anomalously low winter ice coverage in Baffin/Hudson Bay, Davis Strait, the Labrador Sea, and Gulf of Saint Lawrence (Fig. 3D). The increase of humidity in autumn provides an additional local moisture source to Europe, in addition to circulation change induced moisture transport from mid-latitudes through shifting the storm track southward and increasing storminess over the Mediterranean (Fig. 2A). Meanwhile, cold air masses that develop over central Siberia more readily spill over into Europe. Thus, in Europe, it is more likely to see anomalously snowstorm events during late autumn and early winter, which was the case for recent winters. Similarly, the increase of humidity in winter provides an extra local moisture source to northeastern North America. Together with enhanced cold air outbreaks in the eastern and mid-west United States, this increases the likelihood of anomalously snowstorm events in the northeastern and mid-west United States in winter and even persisting into early spring.

The ERA-interim reanalysis also suggests that the largest specific humidity increase during 1989-2008 is in the Arctic region, and a large portion of this enhanced moisture flux is contributed to diminishing Arctic sea ice through surface latent heat flux (27). Moreover, a recent study examined the predominant origin of water vapor in northern high latitudes during the ice growth period using water isotopes (deuterated water, HDO and heavy oxygen water,

1 H_2^{18}O) as tracers, i.e. isotopic values of water vapor originating from the Arctic Ocean have
2 higher d-excess values than those of water vapor originating from lower latitudes, where d-
3 excess value is defined as HDO minus H_2^{18}O . The high d-excess values of Arctic-origin air
4 masses were observed in mid-autumn, and gradually decreased to the global average in early
5 winter (28). This further indicates that the moisture source in Europe (northeastern North
6 America) might be primarily locally driven in late autumn and early winter (winter), and
7 switches from locally driven to moisture transport from lower latitudes in early winter (late
8 winter). Note that specific humidity decreases associated with the reduction of sea ice in the
9 northwestern United States and eastern China, although above-normal snow cover is observed
10 there linked to the reduction of sea ice. This suggests that the moisture source for these regions
11 might primarily come from lower latitudes.

12 To confirm the robustness of the changes of atmospheric circulation and water vapor
13 content linked to the reduction of sea ice identified using the NCEP2 (atmospheric model only
14 reanalysis), we repeat the above analyses using a new reanalysis, the NCEP Climate Forecast
15 System Reanalysis (CFSR, executed in a coupled atmosphere-ocean-sea ice system). As
16 shown in supplementary Fig. 6, the regression patterns of SLP, SAT, and specific humidity of
17 the CFSR closely resemble to those of NCEP2.

18 To further interpret the observational data analyses, we conduct simulations with the
19 National Center for Atmospheric Research Community Atmospheric Model Version 3.1 (29),
20 for which sea surface temperatures (SST) and sea ice concentrations are specified as boundary
21 conditions based on a merged product of the Hadley Centre sea ice and SST data set and the
22 National Oceanic and Atmospheric Administration weekly optimum interpolation SST
23 analysis (30). The simulation configuration has a horizontal resolution of $\sim 2.8^\circ$ degree and 26
24 vertical levels extending up to 3.5-hPa. The impact of the diminishing Arctic sea ice during
25 the freeze-up on atmospheric circulation is assessed by comparing two experiments with
26 different seasonally varying sea ice distributions, with all other external variables held fixed.
27 The control experiment is run with a seasonally varying Arctic sea ice based on the

climatology of the Hadley Centre sea ice concentrations for 1979-2010. The perturbed experiment is integrated with prescribed sea ice loss in autumn and winter based on regressions of the satellite-derived autumn and winter Arctic sea ice concentrations obtained from the National Snow and Ice Data Center, respectively, on the standardized autumn Arctic sea ice index for 1979-2010 that are statistically significant at the 90% confidence level (Fig. 4A and 4B). Thus, the prescribed winter sea ice anomalies can be considered as the autumn sea ice anomalies persisting into winter. Global SSTs in both experiments are set to their climatological monthly values based on the merged SST data set for the same period of record used for the sea ice climatology in the control experiment. In addition, in the perturbed experiment, in those areas where sea ice is removed, SST is set to freezing point of seawater, -1.8°C. To help gauge confidence in the model response's to sea ice losses, each experiment consists of 20 ensemble members with slightly different initial conditions. The response of the model to the prescribed sea ice losses is examined by differencing SLP and SAT between the ensemble mean of the perturbed and control experiments.

As shown in Fig. 4C and 4D, the diminishing Arctic sea ice does induce positive SLP anomalies over high latitudes and negative SLP anomalies over mid-latitudes in winter, which is accompanied by a significant surface warming in the Arctic Ocean, Greenland/northeastern Canada, and cooling over northern North America, Europe, Siberia, and eastern Asia. Moreover, in late autumn and early winter, the regions showing the largest increase of specific humidity are found in Europe (Fig. 4E), whereas during winter it is mainly located in northeastern North America (Fig. 4F). While the regional details differ somewhat between the response of the modeled snowfall (Supplementary Fig. 7) and the observation (Fig. 1B), the model simulation does show above-normal winter snowfall in large parts of the northern United States, central Europe, and northern and central China. The encouraging consistency between model simulations and observations support the hypothesis outlined above.

Discussion

The results of this study add to an increasing body of both observational and modeling

evidence that indicates diminishing Arctic sea ice plays a critical role in driving recent cold and snowy winters over large parts of North America, Europe and East Asia. The relationships documented here illustrate the rapid loss of sea ice in summer and delayed recovery of sea ice in autumn modulates not only winter mean statistics, i.e. snow cover and temperature, but also the frequency of occurrence of weather events, i.e. cold air outbreaks. While natural chaotic variability remains a component of mid-latitude atmospheric variability, recent loss of Arctic sea ice, with its signature on mid-latitude atmospheric circulation, may load the dice in favor of snowier conditions in large parts of northern mid-latitudes. The relationships elucidated here can be also of practical use in seasonal forecasting of snow and temperature anomalies over northern continents and assessing the potential risk of such events. If the decline of Arctic sea ice continues as anticipated by climate modeling results (31, 32), we speculate that episodes of the aforementioned circulation change will become more frequent, along with more persistent snowstorms over northern continents during winter. Year-to-year variations in autumnal sea ice area may provide a useful predictor of wintertime snowfall in these regions. Better understanding of interactions between the diminishing Arctic sea ice, and dominant modes of climate variability (i.e., NAO/AO, El Niño) and natural chaotic variability of the general circulation is fertile area for further research, given the potential to improve seasonal forecasts.

Methods

The Arctic sea ice is obtained from the National Snow and Ice Data Center, which is retrieved from the Scanning Multichannel Microwave Radiometer and the Special Sensor Microwave/Imager using a team algorithm (33). The snow cover is obtained from the Rutgers University Rutgers University Global Snow Lab, which has developed a satellite snow extent climate record back to late 1966 (<http://climate.rutgers.edu/snowcover>). The sea level pressure, surface air temperature, 500-hPa geopotential height, and specific humidity (from surface to 700-hPa) are obtained from the National Center for Environmental Prediction reanalysis II (NCEP2, 34), and the NCEP Climate Forecast System Reanalysis (CFSR, 35).

Preliminary analysis indicates the CFSR is far superior in most respects to the reanalysis of the mid-1990s in both scope and quality, because it is executed in a coupled mode with a more modern data assimilation system and forecast model (35).

Blocking involves the formation of quasi-stationary, long-lived (> 7 days), closed anticyclonic circulation that temporarily divert the prevailing westerly flow of air in troposphere. Here blocking events are defined as intervals in which daily 500-hPa height from the NCEP2 reanalysis exceeds 1 standard deviation about its mean for five consecutive days (36). Cold air outbreaks often occur downstream of high-latitude blocking anticyclones. Here the cold events are defined as daily minimum temperature from the NCEP2 reanalysis 1.5 standard deviation below the climatological mean (36).

We regress winter mean anomaly fields upon the detrended autumn Arctic sea ice area anomaly time series and display the resulting regression coefficients. The amplitudes shown in the regression maps therefore correspond to anomaly values in that field that occur in association with one million km² anomaly in the autumn Arctic sea ice area and can thus be considered typical amplitudes.

Acknowledgments: This research is supported by NASA NEWS, NSF Polar Programs (0838920), 973 program (2011CB309704, 2009CB421406), and NSFC (41176169).

References

1. WMO statement on the status of the global climate in 2008, WMO-No.1039.
2. WMO statement on the status of the global climate in 2009, WMO-No.1055.
3. WMO statement on the status of the global climate in 2010, WMO-No.1074.
4. Solomon S et al. (2007) *Climate Change 2007: The Physical Science Basis* (Cambridge Univ. Press).
5. Symon C, Arris L, Heal B (2004) *Arctic Climate Impact Assessment* (Cambridge Univ. Press).
6. Seager R, Kushnir Y, Nakamura J, Ting M, Naik N (2010) Northern Hemisphere winter snow anomalies: ENSO, NAO and the winter of 2009/10. *Geophys. Res. Lett.*,

37:doi:10.1029/2010GL043830.

7. Ratnam J, Behera S, Masumoto Y, Takahashi K, Yamagata T (2011) Anomalous climatic conditions associated with the El Niño Modoki during boreal winter of 2009. *Clim. Dyn.*, 10.1007/s00382-011-1108-z.
8. Cohen J, Foster J, Barlow M, Saito K, Jones J (2010) Winter 2009-2010: A case study of an extreme Arctic Oscillation event. *Geophys. Res. Lett.*, 37:10.1029/2010GL044256.
9. Thompson D, Wallace J (2000) Annular modes in the extratropical circulation. Part I: Month-to-month variability. *J. Clim.*, 13:1000-1016.
10. Holland M, Bitz C, Tremblay B (2006) Future abrupt reductions in the Summer Arctic sea ice. *Geophys. Res. Lett.*, 33:10.1029/2006GL028024.
11. Serreze M, Holland M, Stroeve J (2007) Perspectives on the Arctic's shrinking sea-ice cover. *Science*, 315:1533-1536.
12. Wang M, Overland J (2009) A sea ice free summer Arctic within 30 years? *Geophys. Res. Lett.*, 36:10.1029/2009GL037820.
13. Alexander M, Bhatt U, Walsh J, Timlin M, Miller J, Scott J (2004) The atmospheric response to realistic Arctic sea ice anomalies in an AGCM during winter. *J. Clim.*, 17:890-905.
14. Magnusdottir G, Deser C, Saravanan R (2004) The effects of North Atlantic SST and sea ice anomalies on the winter circulation in CCM3. Part I: Main features and storm track characteristics of the response. *J. Clim.*, 17:857-876.
15. Deser C, Magnusdottir G, Saravanan R, Phillips A (2004) The effects of North Atlantic SST and sea ice anomalies on the winter circulation in CCM3. Part II: Direct and indirect components of the response. *J. Clim.*, 17:877-889.
16. Singarayer J, Bamber J, Valdes P (2006) Twenty-first-century climate impacts from a declining Arctic sea ice cover. *J. Clim.*, 19:1109-1125.
17. DeWeaver E, Bitz C, Tremblay L (2008) Arctic Sea Ice Decline: Observations, Projections, Mechanisms, and Implications (Geophysical Monograph, American

Geophysical Union), pp268.

18. Kumar A et al. (2010) Contribution of sea ice loss to Arctic amplification. *Geophys. Res. Lett.*, 37:10.1029/2010GL045022 (2010).
19. Deser C, Tomas R, Alexander M, Lawrence D (2010) The seasonal atmospheric response to projected Arctic sea ice loss in the late 21st century. *J. Clim.*, 23:333-351.
20. Honda M, Inoue J, Yamane S (2009) Influence of low Arctic sea-ice minima on anomalously cold Eurasian winters. *Geophys. Res. Lett.*, 36:10.1029/2008GL037079.
21. Ghatak D, Frei A, Gong G, Stroeve J, Robinson D (2010) On the emergence of an Arctic amplification signal in terrestrial Arctic snow extent. *J. Geophys. Res.*, 115:10.1029/2010JD014007.
22. Comiso J, Parkinson C, Gersten R, Stock L (2008) Accelerated decline in the Arctic sea ice cover. *Geophys. Res. Lett.*, 35:10.1029/2007GL031972.
23. Stroeve J, Holland M, Meier W, Scambos T, Serreze M (2007) Arctic sea ice decline: Faster than forecast. *Geophys. Res. Lett.*, 34:10.1029/2007GL029703.
24. Perovich D, Richter-Menge J, Jones K, Light B (2008) Sunlight, water, and ice: Extreme Arctic sea ice melt during the summer of 2007. *Geophys. Res. Lett.*, 35:10.1029/2008GL034007.
25. Jackson J, Carmack E, McLaughlin F, Allen S, Ingram R (2010) Identification, characterization, and change of the near surface temperature maximum in the Canada Basin, 1993-2008. *J. Geophys. Res.*, 115:10.1029/2009JC005265.
26. Overland J, Wang M (2010) Large-scale atmospheric circulation changes associated with the recent loss of Arctic sea ice. *Tellus*, 62A:1-9.
27. Screen J, Simmonds I (2010) The central role of diminishing sea ice in recent Arctic temperature amplification. *Nature*, 464:1334-1337.
28. Kurita N (2011) Origin of Arctic water vapor during the ice-growth season. *Geophys. Res. Lett.*, 38:10.1029/2010GL046064.
29. Collins W et al. The formulation and atmospheric simulation of the Community

- 1 Atmosphere Model Version 3 (CAM3). *J. Clim.*, 19:2144-2161.
- 2 30. Hurrell J, Hack J, Shea D, Caron J, Rosinski J (2008) A new sea surface temperature and
- 3 sea ice boundary dataset for the Community Atmosphere Model, *J. Clim.*, 21:5145-5153.
- 4 31. Arzel O, Fichet T, Goosse H (2006) Sea ice evolution over the 20th and 21st centuries
- 5 as simulated by current AOGCMs. *Ocean Modelling*, 12:401-415.
- 6 32. Holland M, Serreze M, Stroeve J (2010) The sea ice mass budget of the Arctic and its
- 7 future change as simulated by coupled climate models. *Clim. Dyn.*, 34:10.1007/s00382-
- 8 008-0493-4.
- 9 33. Fetterer F, Knowles K, Meier W, Savoie M (2002, updated 2009) Sea Ice Index. Boulder,
- 10 Colorado USA: National Snow and Ice Data Center. Digital media.
- 11 34. Kanamitsu M et al. (2002) NCEP/DOE AMIP-II Reanalysis (R-2). *Bull. Amer. Meteor.*
- 12 *Soc.*, 83:1631-1643.
- 13 35. Saha S et al. (2010) The NCEP climate forecast system reanalysis. *Bull. Amer. Meteor.*
- 14 *Soc.*, 91:1015-1057.
- 15 36. Thompson D, Wallace J (2001) Regional Climate Impacts of the Northern Hemisphere
- 16 Annular Mode. *Science*, 293:85-89.

17 **Figure Legends**

18 Fig. 1. (A) Time series of actual and detrended autumn Arctic sea ice area anomaly ($\times 10^6$
19 km^2), and winter AO index, and (B) linear regression of winter snow cover anomalies (%)
20 on the detrended autumn Arctic sea ice area anomaly (regions within contours denote the
21 regression above 95% confidence level)

22 Fig. 2. Linear regression of winter sea level pressure (hPa, upper panel) and surface air
23 temperature ($^{\circ}\text{C}$, lower panel) on (A, C) the detrended autumn Arctic sea ice area
24 anomaly (regions within contours denote the regression above 95% confidence level), and
25 (B, D) AO index

26 Fig. 3. (A) Ratio (%) between linear regression of incidence of winter blockings on the
27 detrended autumn Arctic sea ice area anomaly and winter blocking climatology during

1 1979-2010, (B) is similar to (A) except for winter cold events, and linear regression of
2 specific humidity (integrated from surface to 700-hPa, kg/kg) in (C) November-December
3 (late autumn to early winter) and (D) December-January (winter) on the detrended autumn
4 Arctic sea ice area anomaly (regions within contours denote the regression above 95%
5 confidence level)

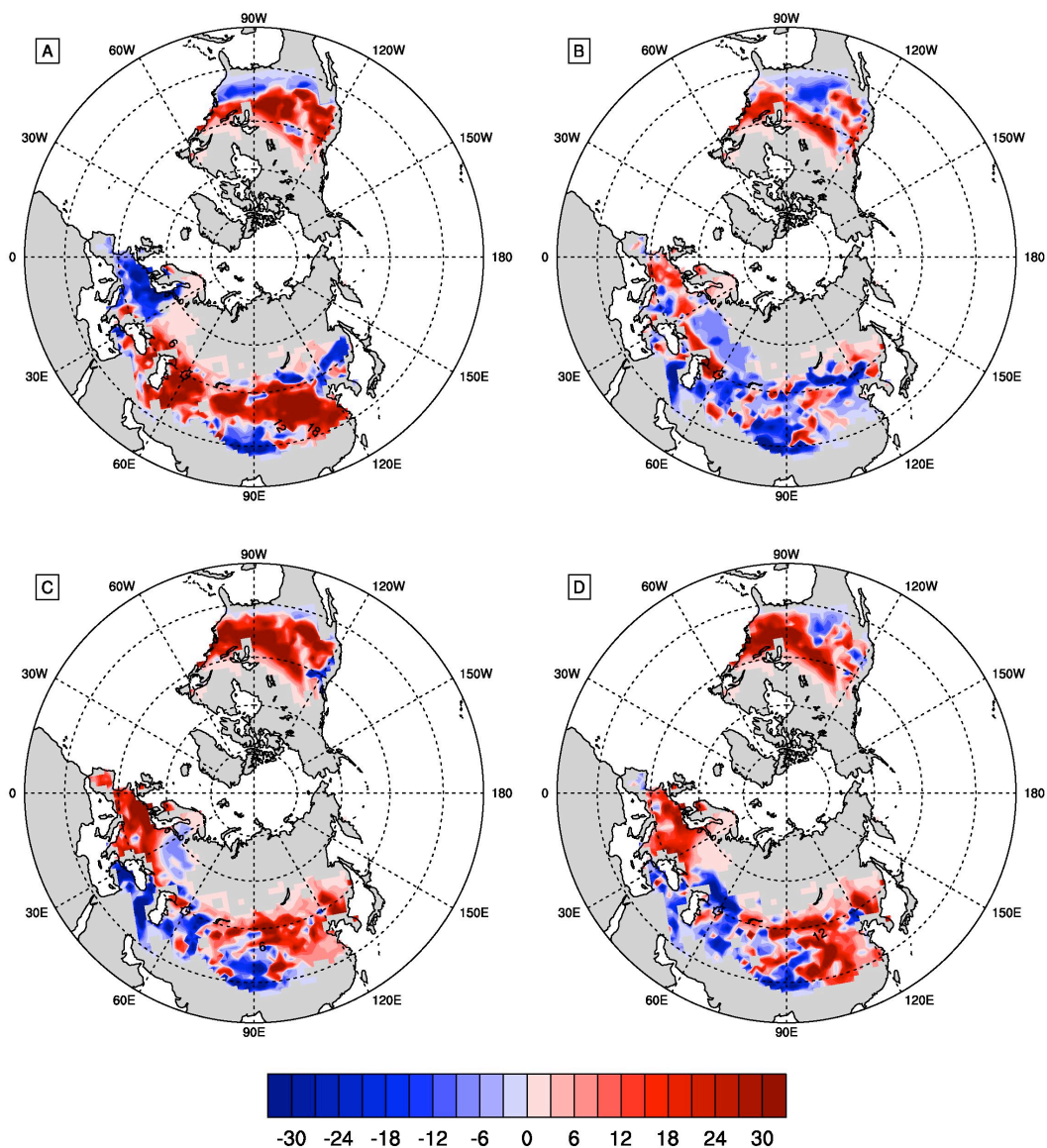
6 Fig. 4. Prescribed sea ice loss (%) in (A) autumn and (B) winter applied to the perturbed
7 experiment, and differences in (C) sea level pressure (hPa) and (D) surface air
8 temperature (°C) in winter, and specific humidity (integrated from surface to 700-hPa,
9 kg/kg) in (E) November-December (late autumn to early winter) and (F) December-
10 January (winter) between the perturbed and control experiments (regions within contours
11 denote the model responses that are above 95% confidence level) \

Impact of Declining Arctic Sea Ice on Winter Snowfall

Jiping Liu,* Judith A. Curry, Huijun Wang, Mirong Song, Radley M. Horton

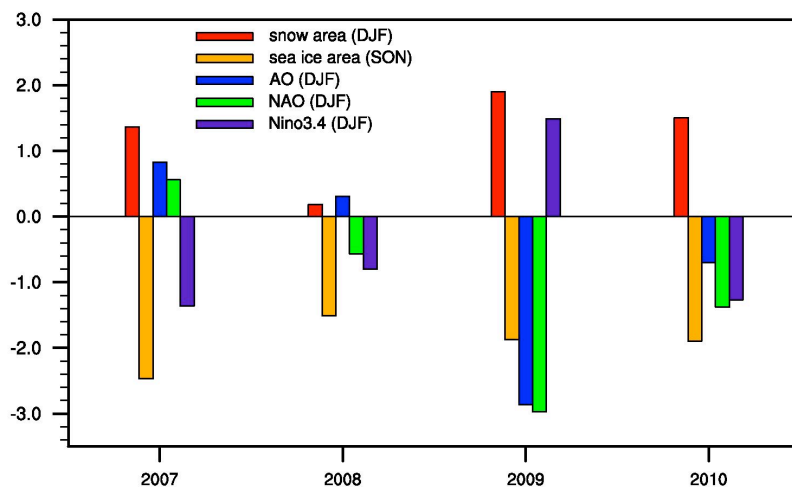
*To whom correspondence should be addressed. Email: jliu@eas.gatech.edu

Supplementary Figures



Supplementary Fig. 1: Spatial distribution of snow cover anomalies (%) for the winter (A) 2007/2008, (B) 2008/2009, (C) 2009/2010, (D) 2010/2011

1



2

3 **Supplementary Fig. 2:** Standardized winter snow area (north of 35°N), autumn Arctic sea ice area, winter
 4 AO, NAO and Nino3.4 for 2007/2008, 2008/2009, 2009/2010, and 2010/2011 (the AO, NAO
 5 and Nino3.4 indices are obtained from <http://www.esrl.noaa.gov/psd/data/climateindices>)

6

7

8

9

10

11

12

13

14

15

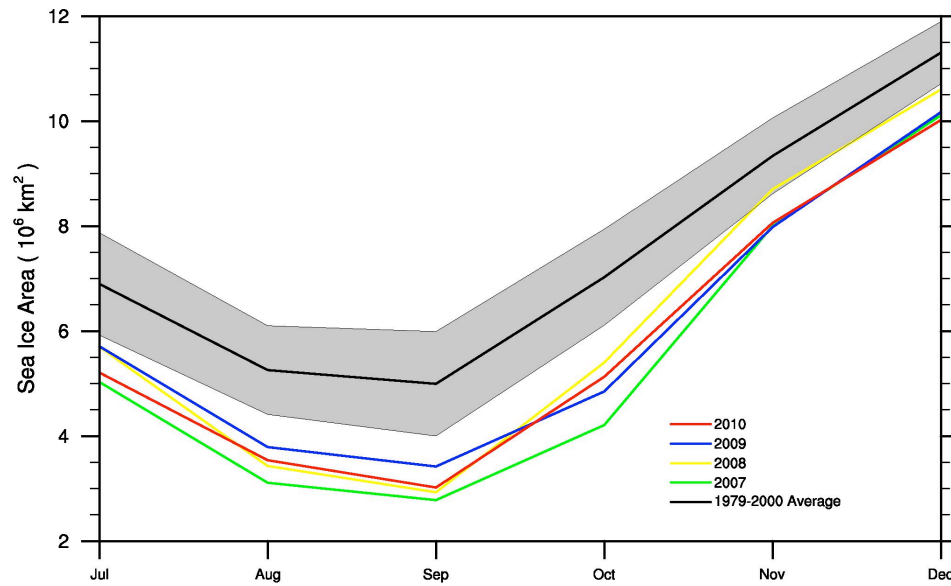
16

17

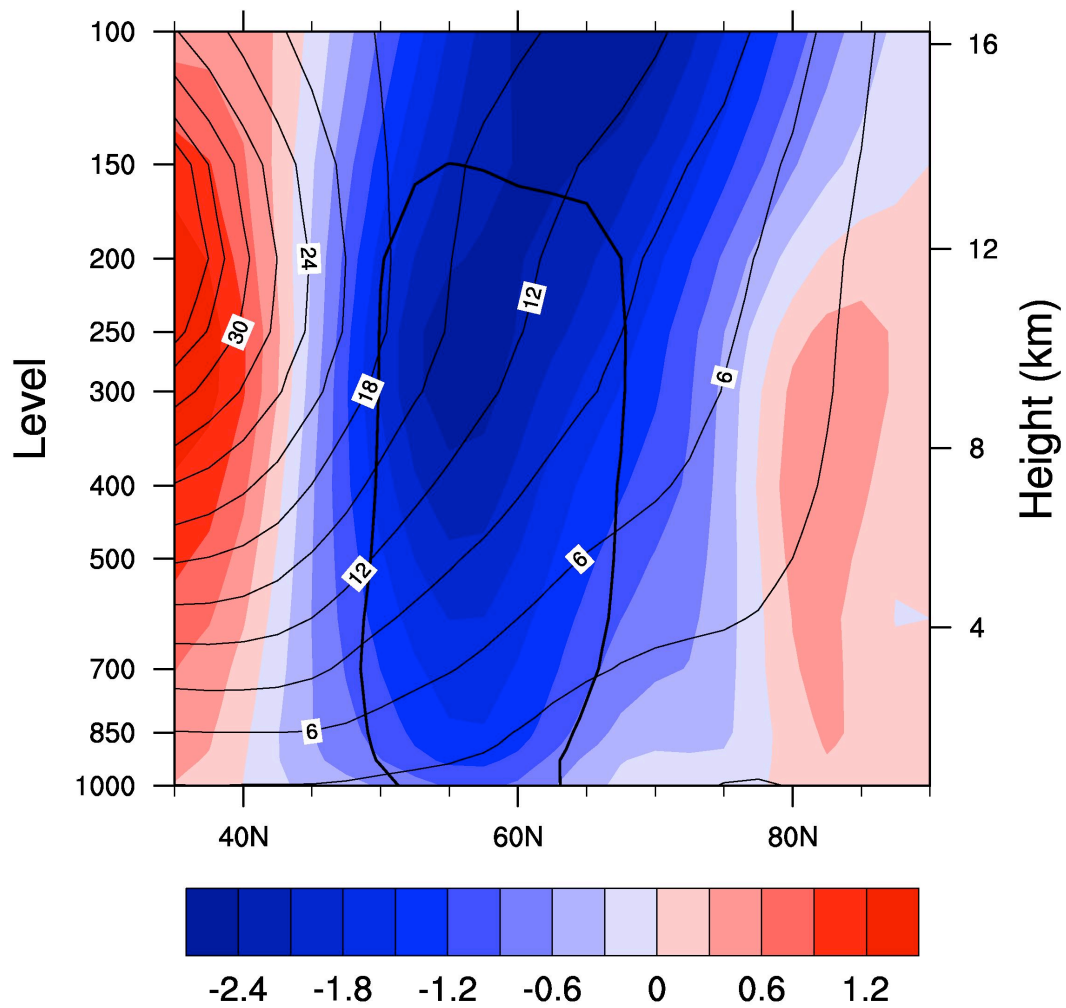
18

19

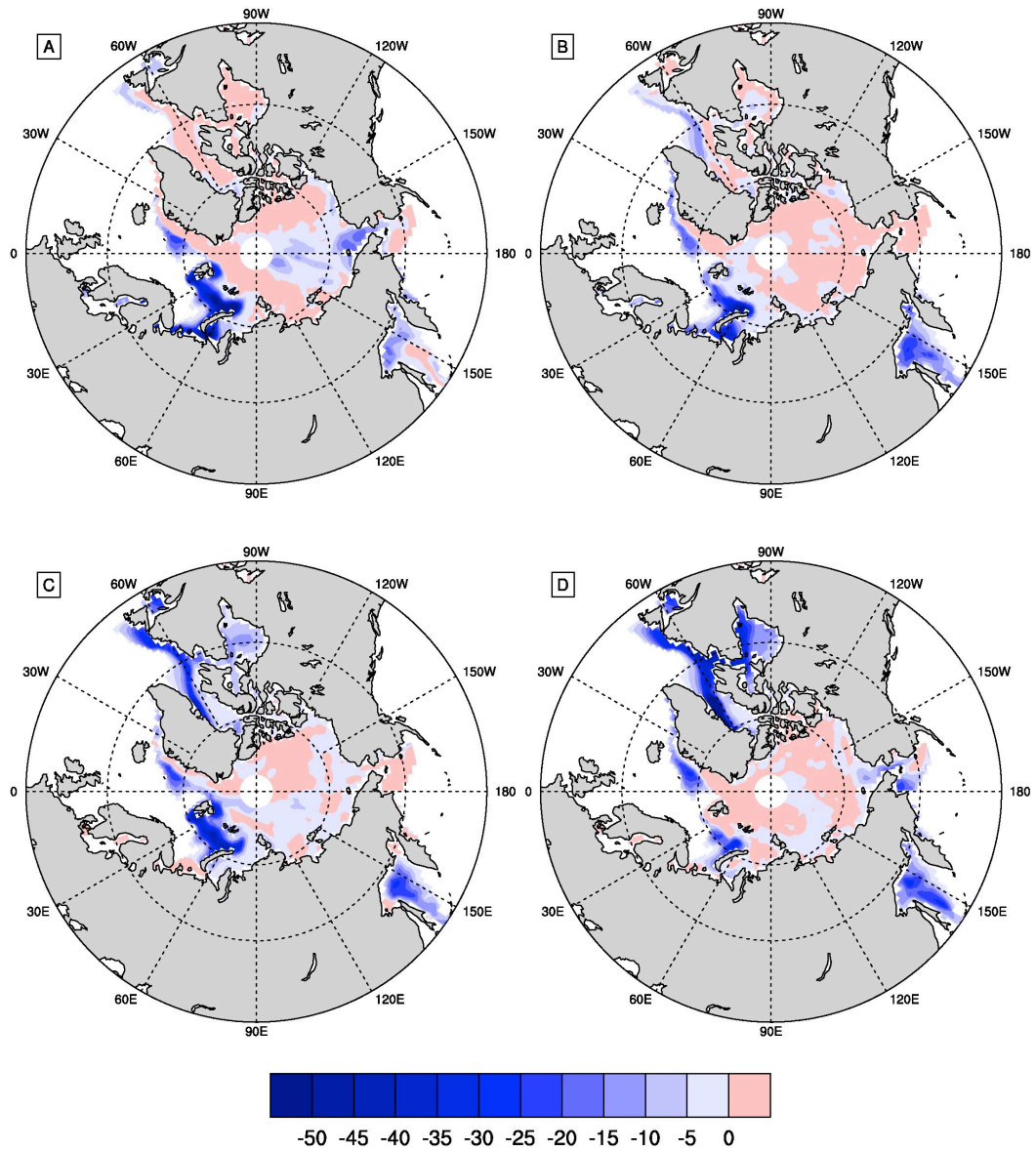
20



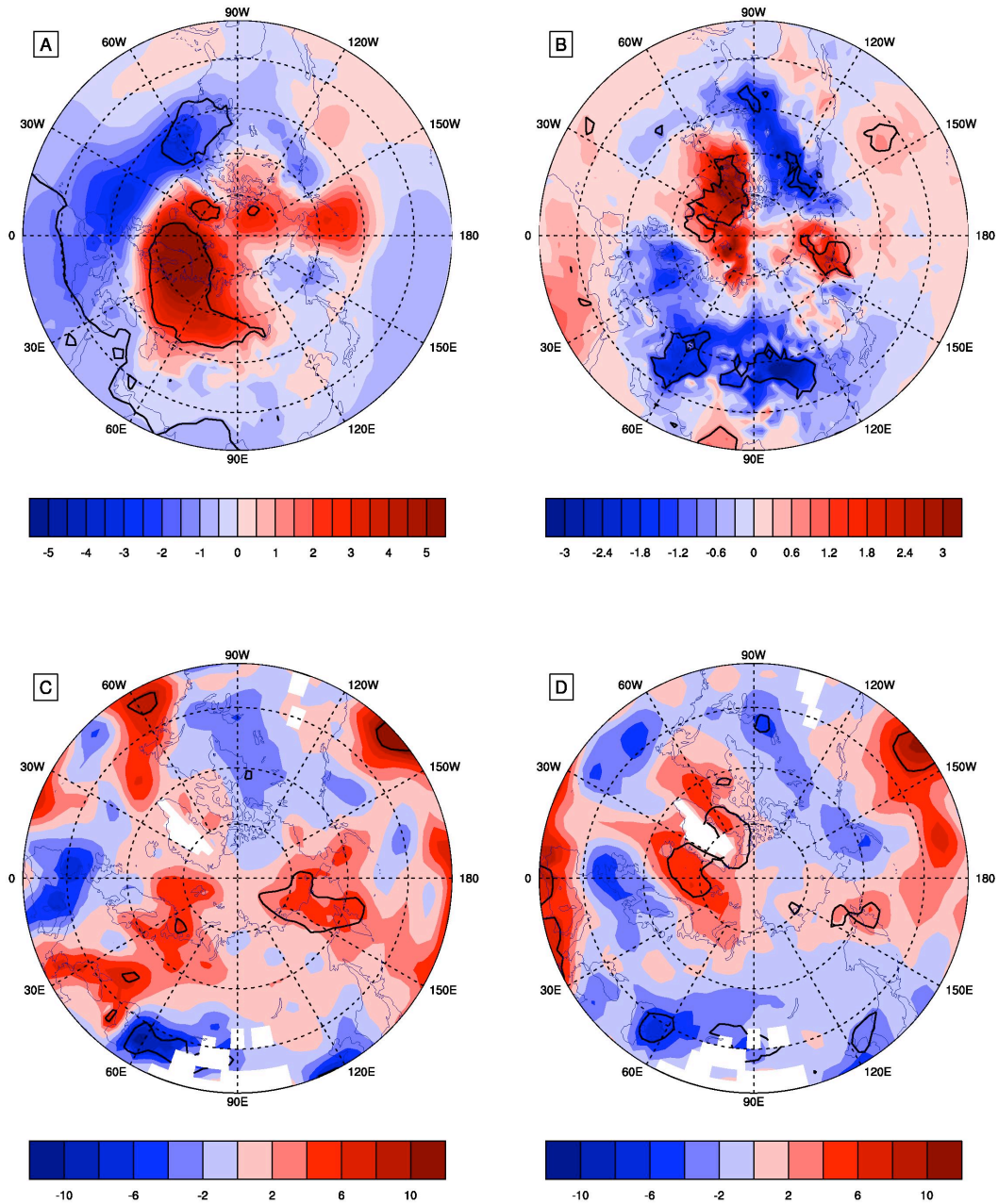
Supplementary Fig. 3: Evolution of Arctic sea ice area ($\times 10^6 \text{ km}^2$) from July to December for 1979-2000 average, 2007, 2008, 2009 and 2010 (the gray area around the 1979-2000 average line denotes the two standard deviation range of sea ice area)



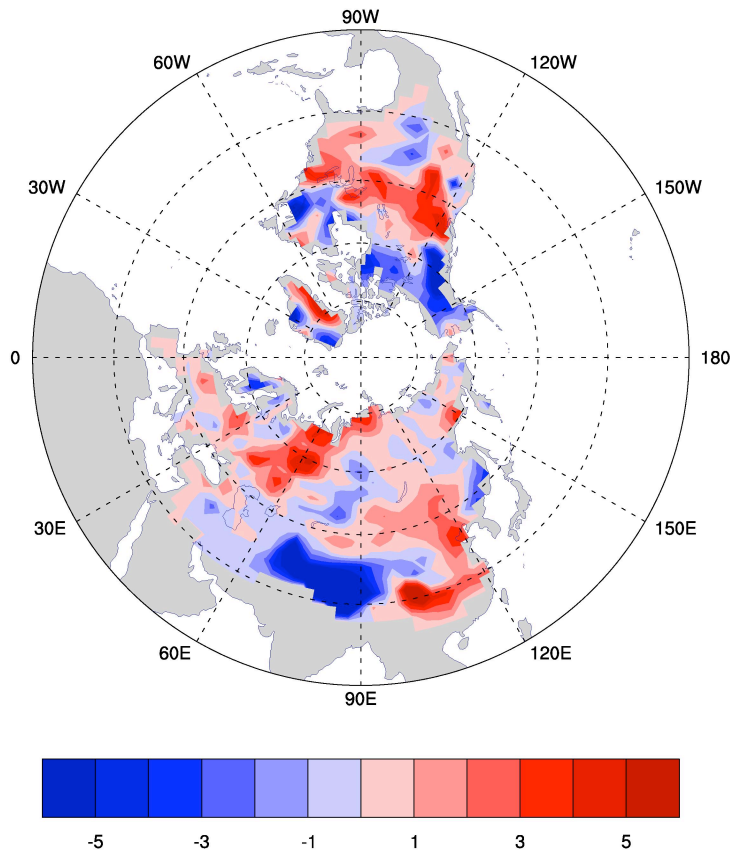
Supplementary Fig. 4: Vertical cross-section of linear regression of the winter zonal mean zonal wind anomalies (color, m/s) on the detrended autumn Arctic sea ice area anomaly (the area within the thick solid contour denote the regression above 95% confidence level). The corresponding climatological zonal mean zonal wind for 1979-2010 is also shown in thin solid contour.



Supplementary Fig. 5: Spatial distribution of sea ice concentration anomalies (%) for the winter (A) 2007/2008, (B) 2008/2009, (C) 2009/2010, (D) 2010/2011



Supplementary Fig. 6: Linear regression of (A) sea level pressure (hPa) and (B) surface air temperature ($^{\circ}\text{C}$) in winter, and specific humidity (integrated from surface to 700-hPa, kg/kg) in (C) November-December (late autumn to early winter) and (D) December-January (winter) for CFSR on the detrended autumn Arctic sea ice area anomaly (regions within contours denote the regression above 95% confidence level)



1

2 Supplementary Fig. 7: Differences in snowfall (mm/month) in winter between the perturbed
 3 and control experiments
 4

5